

## Valence band of $\gamma$ -cerium studied by ultraviolet and x-ray photoemission spectroscopy

A. Platau and S.-E. Karlsson

*Department of Physics and Measurement Technology, Linköping University, S-581 83 Linköping, Sweden*

(Received 18 April 1978)

At room temperature and low pressure, pure cerium is known to be in the  $\gamma$  phase with electron configuration  $4f^1(5d6s)^3$ . When it is compressed to about 7 kbar, a  $\gamma$ - $\alpha$  phase transition occurs. To understand this phase transition, the energy position of the  $f$  level in  $\gamma$ -cerium is of utmost importance. However, it has not been possible to determine an experimental value of the  $f$ -level binding energy using photoemission. In spectra excited by monochromatized Al  $K\alpha$  radiation, the overlapping  $4f$  and  $5d6s$  emissions are not resolved, and it has not been found possible to draw firm conclusions as to the relative order of the  $f$  level and the  $s$ - $d$  band from the structure observed. The present paper concerns ultraviolet-photoemission (UPS) ( $\text{He I}$  and  $\text{He II}$ ) and XPS ( $\text{Mg } K\alpha$ ) measurements on clean Ce films ( $\gamma$ -phase). Even though the  $4f$ -level and  $5d6s$ -band emissions are not resolved, the  $4f$ -level energy position can be estimated from comparison of XPS and UPS valence-band spectra. In the spectra from Ce films exposed to oxygen at room temperature the emission from the  $5d6s$  band is vanishing, thus allowing for an identification of the  $4f$ -level emission. The observed binding energy of the  $4f$  level in  $\gamma$ -Ce is  $1.9 \pm 0.2$  eV relative to the Fermi level. To account for the  $\gamma$ - $\alpha$  phase transition using either the promotion model and its various extensions or the  $sd$ - $f$  hybridization model, it is required that the  $4f$  level is situated just below the Fermi energy in  $\gamma$ -Ce. Thus, the present results disfavor these models. However, in the model describing the  $\gamma$ - $\alpha$  transition as a Mott transition within the  $4f$  shell, such close proximity of the  $4f$  level to the Fermi level is not required. Our results therefore indicate that the  $\gamma$ - $\alpha$  transition is due to a Mott transition of the  $4f$  electron and a subsequent hybridization with the  $sd$  band.

### I. INTRODUCTION

In most of the rare-earth metals there are three electrons in the valence band,  $(5d6s)^3$ , and an integral number of electrons in the localized  $4f$  state. The  $f$  shell gradually becomes filled as one proceeds from lanthanum ( $f^0$ ) to the last element of the series, lutetium ( $f^{14}$ ). Exceptions are europium and ytterbium, with only two electrons in the valence band,  $(5d6s)^2$ , the third one going into the  $f$  shell.

Due to the incomplete screening within the  $f$  shell of the lanthanides, the extension of the  $f$  orbital will decrease monotonically with increasing atomic number. The first metal in the series in which the  $f$  level is occupied is cerium ( $f^1$ ). Therefore, among the lanthanides, cerium will have the spatially most extended  $4f$  orbital.

Cerium has a complicated temperature-pressure phase diagram. When cerium at room temperature is compressed to about 7 kbar, a phase transition takes place from the low-density  $\gamma$  phase to the high-density  $\alpha$  phase. Both  $\gamma$ - and  $\alpha$ -cerium have fcc crystal structure. Both this remarkable isostructure phase transformation as well as other anomalous properties of cerium are certainly due to the behavior of the  $f$  electron. However, exactly how this comes about is at present a controversial question, and various suggestions to account for the  $\gamma$ - $\alpha$  phase transition have been put forward. Thus it has been sug-

gested that (i) it is due to a promotion of the  $f$  electron into the  $sd$  conduction band.<sup>1,2</sup> This picture has been refined in several different ways.<sup>3-5</sup> (ii) It is due to a delocalization of the  $f$  state, i.e., the  $f$  electron undergoes a transition from a localized state into an itinerant  $f$ -band state (a Mott transition within the  $f$  state).<sup>6</sup> (iii) It is due to  $sd$ - $f$  hybridization.<sup>7</sup>

In the different pictures, the position of the  $f$  level in energy and its width are of crucial importance. It is therefore highly desirable that experimental determinations of these parameters be undertaken.

Earlier UPS results on cerium<sup>8</sup> show photoelectrons mainly from the  $5d6s$  band because of the low  $4f$  photoemission cross section for the photon energies used ( $h\nu \leq 11.7$  eV). Recent XPS measurements using soft-x-ray radiation as light source [ $\text{Mg } K\alpha$  (Ref. 9) and monochromatized Al  $K\alpha$  (Refs. 10, 11)] gave electron spectra from the whole valence band,  $4f$  and  $5d6s$ , but the structure observed in the spectra could not be characterized unambiguously. In particular, it was not possible to deduce the relative order of the  $f$  level and the  $sd$  band. Tentatively, however, the binding energy of the  $4f$  level relative to the Fermi level was first given as 1.8 eV,<sup>9</sup> this being subsequently revised to 0.9 eV.<sup>10</sup> Recently, the  $4f$ -level position was placed at 0.5 eV,<sup>11</sup> as concluded from XPS measurements on Al-La, Al-Ce alloys and on La, Ce, and Al metals. However,

the underlying assumptions motivating the evaluation of the data, such as, e.g., studying difference spectra between alloys and pure metals, are not discussed in detail and they are far from obvious.

Thus until now, it has not been possible to locate the energy position of the  $4f$  level in  $\gamma$ -Ce unambiguously by photoelectron spectroscopy.<sup>12</sup> However, by studying the oxidation of cerium by UPS and XPS, we have, in the present work, found strong experimental evidence for a correct identification of the  $4f$ -level photoelectron emission. Thus we can actually determine the energy position and experimental halfwidth of the  $4f$  level.

This paper concerns the valence band of cerium studied by UPS (He I and He II) and XPS (Mg  $K\alpha$ ). The successive oxidation is only used here to differentiate the  $f$  level from the  $sd$  valence band. The detailed oxidation properties of the cerium surface and core-level XPS studies will be reported elsewhere.

## II. EXPERIMENTAL PROCEDURES

The measurements were performed in an ion-pumped ultrahigh vacuum chamber with a basic pressure of  $10^{-8}$  Pa or better. The electron energy distribution was analyzed by a retarding field electron spectrometer with differential output.<sup>13</sup> The resolution of the analyzer was chosen to be between 0.09 and 0.21 eV when operating in the UPS mode and 0.33 eV in the XPS mode. The Au  $4f_{7/2}$  level excited by Mg  $K\alpha$  gave a peak of 0.96 eV FWHM (full width at half maximum). For energy calibration, the Fermi edge of clean Ce metal was used in the UPS studies, while the XPS spectra were calibrated taking the Au  $4f_{7/2}$  line as being located at 83.8 eV binding energy relative to the Fermi level.<sup>14</sup> For excitation of the UPS spectra, a windowless differentially pumped resonance lamp (He I and He II) was used and, for XPS, the Mg  $K\alpha_{1,2}$  doublet from an x-ray tube served as light source. UPS and XPS measurements could be performed on the sample by rotating the sample holder into appropriate positions. The angle between the incident radiation and the direction of electron detection was  $85^\circ$  in UPS and  $90^\circ$  in XPS. The electron-emission angle (defined within  $\pm 3^\circ$  to the surface normal) was  $5^\circ$  for UPS and  $45^\circ$  for XPS measurements.

Cerium metal (99.9%) was evaporated from tungsten filaments, carefully degassed prior to the evaporation, onto a molybdenum substrate that had been polished mechanically ( $3\text{-}\mu\text{m}$  diamond powder). The pressure did not exceed  $10^{-7}$  Pa during evaporation. The initial oxygen contamination was estimated from the O 1s line intensity, only

films containing less than half a monolayer of oxygen being accepted. Repeated evaporations were performed if necessary. Wide scan XPS spectra on the evaporated films showed no trace of other contaminants than the initial oxygen peak. Oxygen exposures were performed at pressures between  $7 \times 10^{-6}$  and  $7 \times 10^{-5}$  Pa, as measured by an ion gauge. The purity of the oxygen was monitored by a quadrupole mass filter. [At a pressure of  $7 \times 10^{-5}$  Pa, only hydrogen ( $<0.5\%$ ), helium ( $<0.1\%$ ), nitrogen and/or carbon monoxide ( $<2\%$ ), and carbon dioxide ( $<1\%$ ) were found in addition to oxygen.] The ion gauge and the mass spectrometer were placed at a moderate distance from, but out of the direct line of sight from, the sample in order to prevent excitation of the oxygen. To permit a heavy oxidation of the Ce film, one oxygen exposure was performed with the sample at approximately  $600^\circ\text{C}$ . All other exposures and all measurements were performed with the sample at room temperature. When running the helium lamp the pressure rose to  $3 \times 10^{-8}$  Pa, but no contaminants other than helium could be detected in the mass spectra.

## III. RESULTS AND DISCUSSION

### A. Valence band of clean cerium

The valence-band spectra excited from clean cerium films by He II and Mg  $K\alpha$  radiations are quite similar (Fig. 1). The shape and total width (2.5 eV) of the Mg  $K\alpha$  induced valence-band spectrum is close to that reported by Steiner *et al.*,<sup>11</sup> although they used monochromatized Al  $K\alpha$ . The He II induced valence-band spectrum has also about the same total width in spite of the better resolution in our UPS measurements. Due to the difference in resolution, the step at the Fermi edge is steeper in UPS (*A*) than in XPS (*A'*). The UPS spectrum of the valence band shows a kind of shoulder (*B*) at 2 eV. On the other hand, in XPS the valence-band spectrum forms a more symmetrical peak. In neither spectrum can the  $f$ -level emission be separated from the  $sd$  band emission. That there is appreciable emission from  $f$  states at He II photon energy (40.8 eV) can be concluded from the energy dependence of the  $4f$  photoabsorption cross section, which has a maximum near a photon energy of 40 eV.<sup>15</sup> However, the relative photoemission cross sections of the  $f$  level and the  $sd$  band,  $\sigma_{4f}/\sigma_{sd}$ , increase with increasing photon energy when going from He II to Mg  $K\alpha$  radiation. Thus, from a comparison of the two spectra, we may interpret structures *A* and *A'* as being due to the  $sd$  band emission and structures *B* and *B'* as being due to the

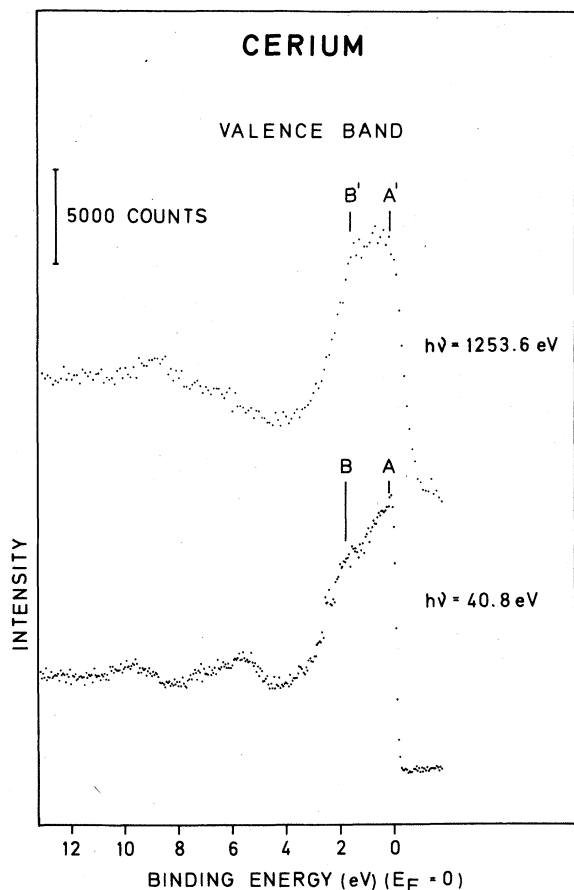


FIG. 1. XPS ( $h\nu=1253.6$  eV) and UPS ( $h\nu=40.8$  eV) valence-band spectra of  $\gamma$ -Ce. The analyzer resolution was set to 0.33 eV in XPS and 0.13 eV in UPS. To normalize the spectra to about the same step height at the Fermi edge, the UPS spectrum is multiplied by 4.5.

$f$  level. However, more convincing experimental evidence for the  $4f$ -level energy position will be given in Sec. III B, in which some results of the oxidation experiments are presented.

To complete the discussion of the spectra shown in Fig. 1, we want to make some comments on the structures seen at binding energies higher than the valence band. The weak structure at 6 eV found in UPS is interpreted as being due to oxygen- $2p$  emission originating from an initial contamination of oxygen (estimated to represent less than 0.1 of a monolayer). It is not seen in XPS because of the lower excitation cross section and lower surface sensitivity. The structure seen at 9 eV in XPS is due to the Ce- $5p$  emission excited by the Mg  $K\alpha_{3,4}$  satellite.

The spectra shown in Fig. 1 were measured on a film which had a very small amount of initial contamination due to oxygen. Different fast evaporations from the same filament and with al-

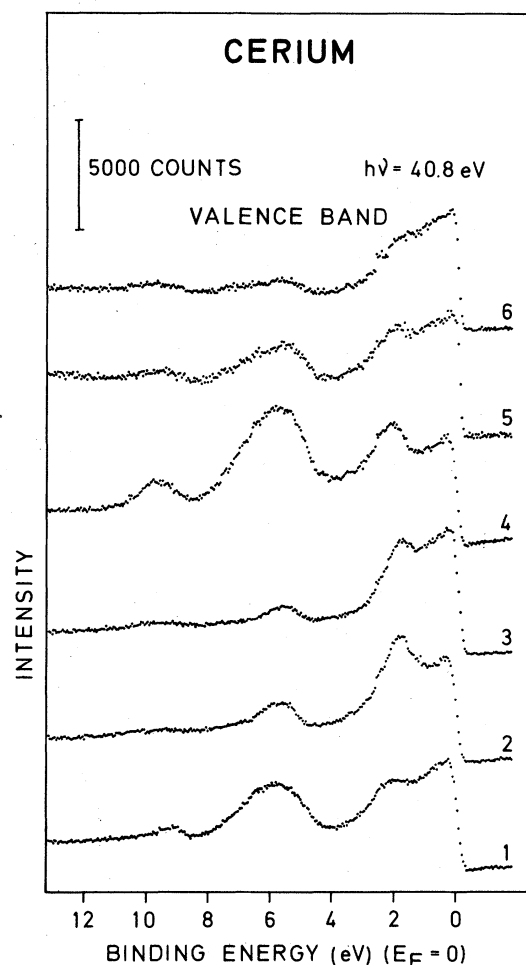


FIG. 2. UPS ( $h\nu=40.8$  eV) valence-band spectra of  $\gamma$ -Ce recorded from six different Ce films. The spectra 1-4 are recorded at 0.21-eV analyzer resolution, while 5 and 6 are recorded at 0.09 and 0.13 eV, respectively. To normalize the spectra to about the same step height at the Fermi edge, the spectra 4-6 are multiplied by 1.5, 2.4, and 1.7.

most the same experimental conditions could lead to films with varying amounts of initial contamination. The He II induced valence-band spectra on six different films are shown in Fig. 2. Roughly speaking, the same total width of the valence band is obtained, but the intensity of the structure at 2 eV varies in comparison to the emission from the vicinity of the Fermi edge. As already mentioned, the peak at around 6 eV is due to O- $2p$  emission and thus gives a rough measure of the initial contamination. Further, it should be noted that the higher the O- $2p$  peak, the less is the emission from the direct vicinity of the Fermi edge. This finding would explain the spectra from films 1 and 4-6. However, films 2 and 3 show,

in comparison, an exceptionally high emission from the  $4f$  peak at 2 eV. Similar variations in XPS valence-band spectra have been reported earlier. As probable explanations, the influence of contamination by oxygen has been discussed, as has the possibility of a different Ce-metal phase at the surface.<sup>10</sup> The influence of oxygen is obvious and easily seen in our UPS results (Fig. 2) by virtue of the higher surface sensitivity together with the higher O- $2p$  emission cross section (in comparison to XPS). Besides the variations in shape caused by oxygen, there could also be a directional effect: different evaporations could result in polycrystalline films with different preferential orientations. It therefore does not seem to be necessary to invoke the existence of a different Ce-metal phase in order to explain the observed variations.

From the spectra in Fig. 2, we thus conclude that the  $4f$ -level energy position in  $\gamma$ -Ce is found at  $1.9 \pm 0.2$  eV.

#### B. Valence band of cerium after different oxygen exposures

Because of the extremely high reactivity of cerium, Ce is the most reactive rare-earth element except for Eu, even "clean" evaporations will result in a certain contamination by oxygen. To clarify the influence of this contamination, systematic surface-oxidation experiments are important. Some results from such experiments, which also throw light on the valence band and the  $4f$ -level positions, are presented here.

Subsequent oxygen exposures were found to change the He II induced spectra (see Fig. 3) in the following manner: (i) A broad peak appears at 6 eV due to O- $2p$  emission from chemically bound oxygen. (ii) The intensity near the Fermi edge is reduced with increasing exposure to oxygen. [Compare the spectrum "clean metal" with (0-L) with the spectra after 1-, 3-, and 10-L oxygen exposure.] Electron emission from the Ce metal is reduced by inelastic scattering within the oxide layer at the surface. (iii) After an exposure of 100 L, only electrons due to the emission from the oxide are detected. The emission from the Fermi edge has disappeared. (iv) The structure at 2 eV does not depend on oxygen exposure apart from a small shift to higher binding energies. The intensity of the peak appears to be independent of oxygen exposure (possible fluctuations may be due to variations of the lamp parameters, pressure, or discharge current, although efforts were made to keep these conditions constant).

The peak at 2 eV with an intensity which does not depend on oxygen exposure is interpreted as being due to the  $4f$  level, and that part of the

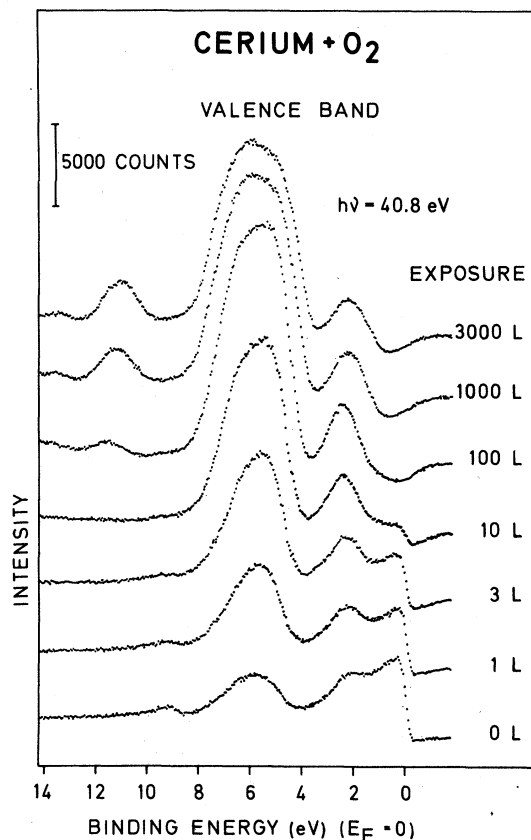


FIG. 3. UPS ( $h\nu = 40.8$  eV) valence-band spectra of Ce after various exposures to oxygen (1 L =  $10^{-6}$  Torr sec). The analyzer resolution was set to 0.21 eV.

valence band which vanishes after appropriate oxygen exposure is interpreted as being emission from the  $(5d6s)^3$  band. This would be consistent with the assumption that no higher oxide than Ce(III) oxide is formed by exposure to oxygen at room temperature.

Thus we draw the following conclusions: (i) The oxide phase formed depletes the Ce  $sd$  band but does not affect the  $4f$  level apart from a small shift to higher binding energies. (ii) The  $4f$  level in the cerium oxide formed is located at  $2.4 \pm 0.2$  eV binding energy with an experimental halfwidth of  $1.2 \pm 0.2$  eV.

The position of the  $4f$  level in  $\gamma$ -Ce metal cannot be concluded solely from the oxidation experiment, because of the unknown chemical shift in the oxide. However, the identification of the  $4f$ -level emission in the oxide, as seen from Fig. 3, gives an estimate of the intensity in the actual experiment. (Compare also the  $4f$  emission in the XPS spectra shown in Fig. 6.) Assuming that the photoemission cross section does not depend strongly on the chemical environment, a  $4f$ -level position of  $1.9 \pm 0.2$  eV in  $\gamma$ -Ce is consistent with

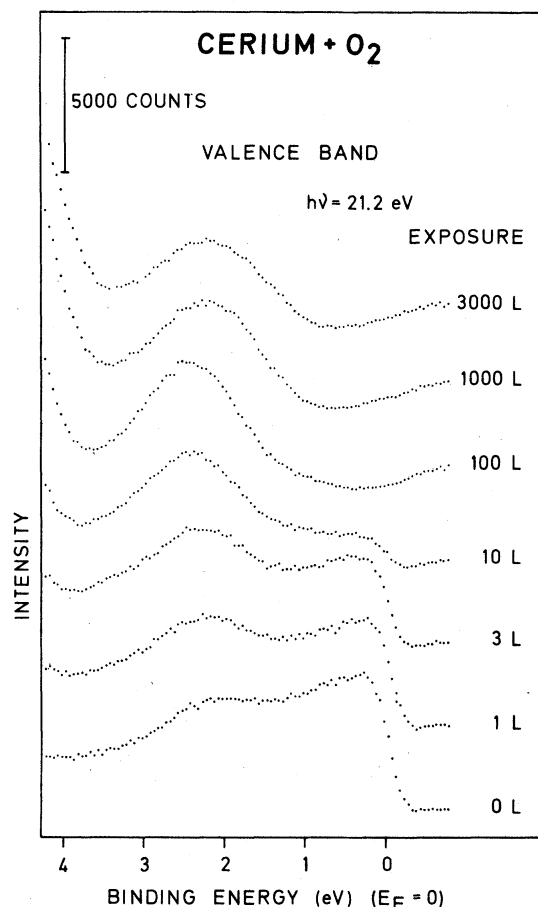


FIG. 4. UPS ( $h\nu = 21.2$  eV) valence-band spectra of Ce after various exposures to oxygen. The analyzer resolution was set to 0.21 eV.

all the XPS and UPS spectra shown.

The UPS results from the He I excitation (see Fig. 4) lead to similar conclusions:  $E_B(4f) = 2.4 \pm 0.2$  eV and a halfwidth of  $1.0 \pm 0.2$  eV FWHM in Ce oxide.

To provide further evidence that the apparently constant peak is due to emission from the 4f level, a new Ce film was prepared, exposed to 1000-L oxygen at room temperature, heated, and then exposed to 1000-L oxygen with the Ce film at approximately 600°C. The He II induced spectra obtained are shown in Fig. 5. The spectra at 0 and 1000 L (room temperature) agree with those presented above. The spectrum obtained after exposure at the elevated temperature shows a reduced Ce-4f emission. This would be consistent with the assumption that Ce(IV) oxide is formed when the oxygen exposure is performed at high temperatures. That there is still a small 4f emission may be due to a Ce excess in CeO<sub>2</sub> or, in other words, due to the existence of oxide

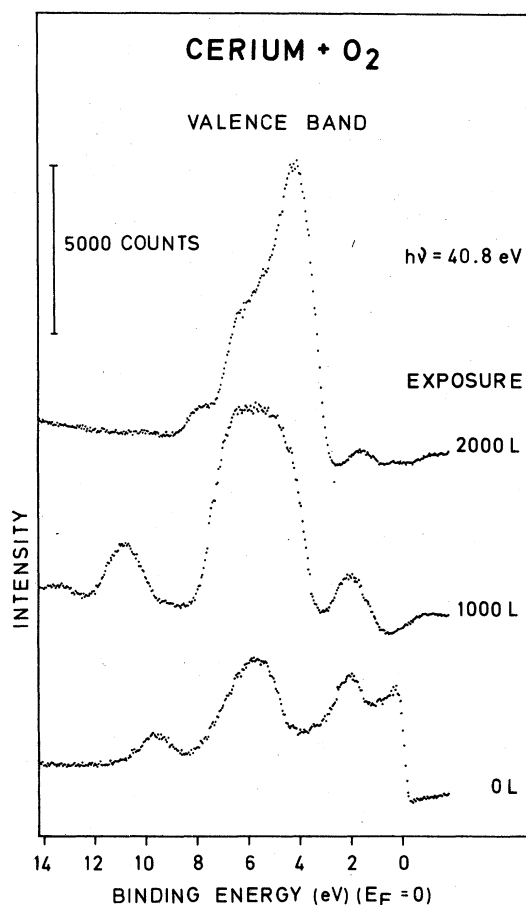


FIG. 5. UPS ( $h\nu = 40.8$  eV) valence-band spectra of  $\gamma$ -Ce and Ce oxides. The resolution of the analyzer was set to 0.21 eV. The spectrum 0 L is taken immediately after evaporation. The initial contamination is estimated to be of the order of 0.5 monolayer. The spectrum 1000 L is taken after exposure to 1000-L oxygen at room temperature. The spectrum 2000 L is taken after further exposure to 1000-L oxygen with the Ce film heated to approximately 600°C. All measurements were performed at room temperature.

phases between Ce<sub>2</sub>O<sub>3</sub> and CeO<sub>2</sub> of the form Ce<sub>n</sub>O<sub>2n-2</sub> ( $n = 4, 7, 9, 10, 11, 12, \dots$ ). The latter oxides are formed at elevated temperatures and insufficient oxygen exposure (for forming pure CeO<sub>2</sub>). Similar behavior has been reported in the oxidation of uranium.<sup>16,17</sup>

Although our Mg  $K\alpha$  induced valence-band spectra taken after different oxygen exposures suffer from poor statistics, we would like to present the spectra here (Fig. 6) to confirm the results and interpretations given above. In this case too, the emission from the vicinity of the Fermi edge is somewhat reduced after an oxygen exposure of 10 L, but not so much as in UPS because of the lower surface sensitivity in XPS. The

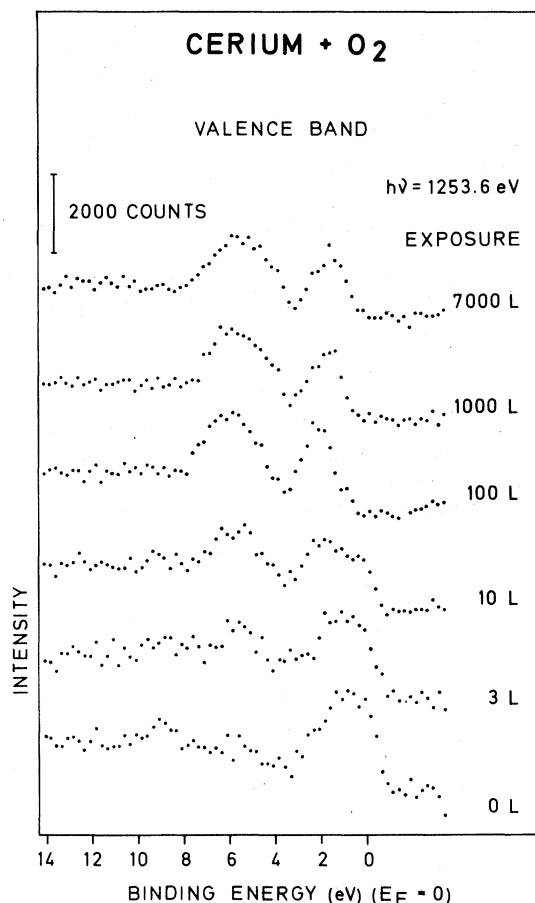


FIG. 6. XPS ( $h\nu=1253.6$  eV) valence-band spectra of Ce after various exposures to oxygen. The analyzer resolution was set to 0.33 eV. The spectra 0, 3, and 1000 L are multiplied by 2, 2, and  $\frac{2}{3}$ , respectively, in order to compensate for different sampling times.

emission from the vicinity of the Fermi edge vanishes for exposures  $\geq 100$  L, but the  $4f$ -level emission is unaffected. The emission from the vicinity of the valence band is interpreted as being due to the  $(sd)^3$  band. From the vanishing of the  $sd$  emission after oxygen exposure, it can be concluded that oxygen interaction leads to the formation of an oxide layer of the form  $Ce_2O_3$ . (Our XPS results on the Ce  $3d$  level from  $Ce_2O_3$ ,  $CeO_2$  powders and Ce film +  $O_2$ , and Ce film +  $O_2$  + heat support this interpretation.)

Because of the vanishing of the  $sd$  emission, the oxide layer thus formed is not protective within the electron escape depth ( $\approx 20$  Å). This interpretation is in contrast to earlier reports.<sup>8,18,19</sup> (A more detailed discussion will be published elsewhere.)

The heavy oxidation at elevated temperatures leads to the formation of  $CeO_2$ , as seen by the

vanishing of the  $4f$  emission (the spectrum is not included here, but compare the reduced  $4f$  emission in UPS, Fig. 5).

The XPS (Fig. 6) and UPS (Figs. 2 and 3) measurements were taken consecutively after various oxygen exposures to permit a characterization of the state of the same surface by both XPS and UPS.

#### IV. CONCLUSION

We believe that we have given experimental evidence for a correct identification of the  $4f$  level in  $\gamma$ -Ce metal. While our results do not contradict earlier valence-band measurements on Ce, they do not agree with the interpretations given concerning the labeling of the bands. The position and width of the  $f$  level agree fairly well with the theoretical calculations by Herbst *et al.*<sup>20</sup> In Ce halides<sup>21</sup> the  $4f$  level is found at 3-eV binding energy (XPS). In light rare-earth antimonides,<sup>22</sup> the  $4f$ -level positions in XPS spectra agree well with those found in the clean metals. Comparison of the spectra of LaSb and CeSb indicates a  $4f$ -level position in CeSb of 3 eV. Thus our result, the finding of a  $4f$ -binding energy of 1.9 eV in  $\gamma$ -Ce, is much more plausible than a position direct at the Fermi edge would be. Final-state effects, such as incomplete relaxation, as discussed by Baer and Busch,<sup>10</sup> cannot be ruled out, but the independence of the  $4f$ -level position on the excitation energy (compare Figs. 1 and 4) gives some indication that final-state effects are of less importance. The value for the  $4f$ -level position reported here is in fact close to that first reported by Baer and Busch,<sup>9</sup> and also agrees with that advanced by Johansson<sup>6,23,24</sup> on thermodynamic reasons.

In the promotion model (and its various extensions), as well as in the  $sd$ - $f$  hybridization model, it is required that the  $4f$  level be situated just below the Fermi energy in the Ce  $\gamma$  phase. Thus the present results disfavor these models. However, in the model describing the  $\gamma$ - $\alpha$  transition as a Mott transition within the  $4f$  shell,<sup>5</sup> such a close proximity of the  $4f$  level to the Fermi level is not required. Therefore, our results give evidence for the view that the  $\gamma$ - $\alpha$  transition is due to a Mott transition of the  $4f$  electron with a subsequent hybridization with the  $sd$  electrons.

#### ACKNOWLEDGMENTS

This work has been financially supported by the Swedish Natural Research Council. The authors wish to thank Professor Stig Hagström for initiation of the project and for constant encouragement.

- <sup>1</sup>H. W. Zachariasen, *J. Inorg. Nucl. Chem.* **35**, 3487 (1973).
- <sup>2</sup>L. Pauling, *J. Chem. Phys.* **18**, 145 (1950).
- <sup>3</sup>B. Coqblin and A. Blandin, *Adv. Phys.* **17**, 281 (1968).
- <sup>4</sup>R. Ramirez and R.M. Falicov, *Phys. Rev. B* **3**, 2425 (1971).
- <sup>5</sup>L. L. Hirst, *J. Phys. Chem. Solids* **35**, 1285 (1974).
- <sup>6</sup>B. Johansson, *Philos. Mag.* **30**, 469 (1974).
- <sup>7</sup>H. H. Hill and E. A. Kmetko, *J. Phys.* **5**, 1119 (1975).
- <sup>8</sup>C. R. Helms and W. E. Spicer, *Appl. Phys. Lett.* **21**, 237 (1972).
- <sup>9</sup>Y. Baer and G. Busch, *Phys. Rev. Lett.* **31**, 35 (1973).
- <sup>10</sup>Y. Baer and G. Busch, *J. Electron Spectrosc. Relat. Phenom.* **5**, 611 (1974).
- <sup>11</sup>P. Steiner, H. Höchst, and S. Hüfner, *J. Phys. F* **7**, L145 (1977).
- <sup>12</sup>Y. Baer and Ch. Zürcher, *Phys. Rev. Lett.* **39**, 956 (1977).
- <sup>13</sup>I. Lindau, J. C. Helmer, and J. Uebbing, *Rev. Sci. Instrum.* **44**, 265 (1973).
- <sup>14</sup>G. Johansson, J. Hedman, A. Berndtsson, M. Klasson, and R. Nilsson, *J. Electron Spectrosc. Relat. Phenom.* **2**, 295 (1973).
- <sup>15</sup>G. Brodén, Thesis, 1972, Göteborg, Sweden, Doktorsavhandlingar vid Chalmers Tekniska Högskola, Ny serie Nr 34.
- <sup>16</sup>B. W. Veal and D. J. Lam, *Phys. Rev. B* **10**, 4902 (1974).
- <sup>17</sup>B. W. Veal and D. J. Lam, *Phys. Lett. A* **49**, 466 (1974).
- <sup>18</sup>C. R. Helms, Thesis, Technical Report No. 5236-1, Stanford (1973).
- <sup>19</sup>A. Platau, L. I. Johansson, A. L. Hagström, S.-E. Karlsson, and S. B. M. Hagström, *Surf. Sci.* **63**, 153 (1977).
- <sup>20</sup>J. F. Herbst, D. N. Low, and R. E. Watson, *Phys. Rev. B* **6**, 1913 (1972).
- <sup>21</sup>S. Sato, *J. Phys. Soc. Jpn.* **41**, 1913 (1976).
- <sup>22</sup>M. Campagna, E. Bucher, G. K. Wertheim, D. N. E. Buchanan, and L. D. Longinotti, Proceedings of the 11th Rare Earth Research Conference, Oct. 7-10, 1974, Traverse City, Michigan, p. 810-819.
- <sup>23</sup>B. Johansson, *Phys. Rev. B* **12**, 3253 (1975).
- <sup>24</sup>B. Johansson, *J. Phys. F* **7**, 877 (1977).